Measurement of Inclusive Two-Particle Angular Correlations in pp Collisions at ATLAS

Cristina Oropeza Barrera* for the ATLAS Collaboration

School of Physics and Astronomy, University of Glasgow, Glasgow, Scotland, UK

Abstract. Measurements of two-particle angular correlations in proton-proton collisions at a centre-of-mass energy of 7 TeV, produced by the Large Hadron Collider, are presented. Correlations are measured for charged particles in the kinematic region $p_T > 100$ MeV and $|\eta| < 2.5$. Collision events were recorded using a minimum bias trigger with the ATLAS Detector at the LHC during 2010. A complex correlation structure in $\Delta\eta$ and $\Delta\phi$ is observed. Results are compared to Pythia 8 and Phojet as well as the ATLAS MC09, DW and Perugia$_0$ tunes of Pythia 6.

Keywords: Two-particle Correlations, Tuning, QCD
PACS: 13.85.Ni, 25.75.Gz

INTRODUCTION

The study of correlations between final state particles is a powerful method for investigating the underlying mechanisms of particle production [1]. Additionally, particle correlations can help to identify important dynamical information that can be incorporated in models or theories to gain a better and more global description of multi-particle production within soft interactions.

This study focuses on the measurement of two-particle angular correlations in pseudorapidity, η, and azimuthal angle, ϕ, and explores their different components using data collected by the ATLAS Inner Detector [2]. The ATLAS note describing in more detail these results can be found in [3]. Events were required to contain at least two tracks in the phase-space defined by $p_T > 100$ MeV and $|\eta| < 2.5$ (which corresponds to an integrated luminosity of 190 μb^{-1}). A comparison of the data to the Monte Carlo generators Pythia 8 [4] and Phojet [5] and different Pythia 6 [6] tunes (DW [7], Perugia$_0$ [8] and MC09 [9]) is also performed.

TWO-PARTICLE CORRELATION FUNCTION

The inclusive two-particle angular correlation function is given by:

$$R(\Delta\eta,\Delta\phi) = \frac{\langle (N_{ch}-1)\,F\,(N_{ch},\Delta\eta,\Delta\phi)\rangle_{ch}}{B\,(\Delta\eta,\Delta\phi)} - \langle N_{ch}-1\rangle_{ch}\,, \tag{1}$$

where $F(N_{ch},\Delta\eta,\Delta\phi)$, the foreground, represents the correlations between emissions in a single event, containing contributions from both correlated and uncorrelated pairs.

The background $B(\Delta\eta, \Delta\phi)$ is used to account for phase-space and detector effects by using the distribution of uncorrelated pairs. Finally, N_{ch} is the average track multiplicity and $\langle ... \rangle_{ch}$ indicates an average over contributions from all particle multiplicities.

In practice, $\langle (N_{ch} - 1) F (N_{ch}, \Delta\eta, \Delta\phi) \rangle_{ch}$ is constructed by taking each pair of particles within a single event, calculating their η and ϕ separations and filling a two-dimensional histogram at those values using a weight of $2/N_{ch}$. This histogram is normalised by dividing each bin by the number of events entering the distribution. The background distribution is determined by taking pairs of independent events and, for each particle in one event, the $\Delta\eta$ and $\Delta\phi$ values with each particle in the other event are calculated and used to fill another two-dimensional histogram. The background two-dimensional histogram is finalised by normalising it to unit integral.

CORRECTION PROCEDURE

The effect of mis-reconstructed tracks is corrected for using a data-driven method that requires knowledge of the single track reconstruction efficiency as a function of track p_T and η. Figure 1 illustrates the correction procedure in which the observable is first computed using all reconstructed tracks satisfying the analysis cuts (solid black line). The track reconstruction efficiency is determined for each track and compared to a random number, generated uniformly between zero and one. If the random number is greater than the track reconstruction efficiency, the track is removed from the sample. Using the remaining subset of tracks, the observable is calculated again. This defines one iteration of the track-removal procedure. A second iteration takes as input the tracks used in the first iteration and again uses a new set of random numbers to remove some tracks according to their track reconstruction efficiency. Further iterations are carried out in the same way.

Each iteration corresponds to an additional application of the detector effect on the data. The value of each bin of the observable can be plotted as a function of the known iteration number (0, 1, 2, ..., 6) and a function can be fitted (3^{rd} degree polynomial) to the resulting distribution as illustrated on the right plot in Figure 1. Such a plot is obtained for each and every bin in the R($\Delta\eta$) distribution. By extrapolating the fit to -1 an estimate of the true observable without detector effects can be made.

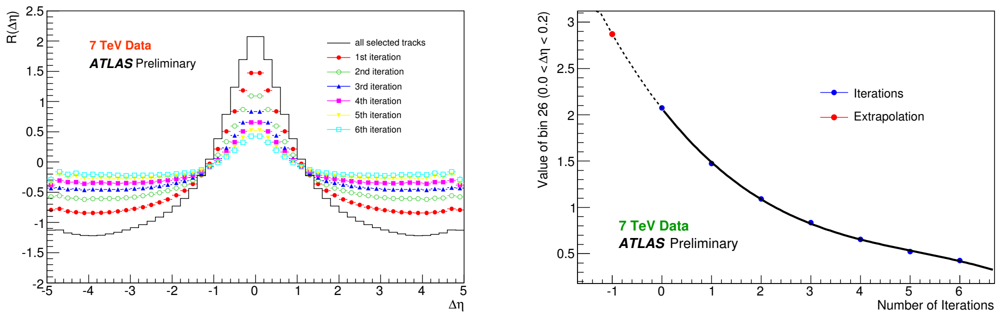

FIGURE 1. Left: two-particle pseudorapidity correlation function after each iteration in the correction method for 7 TeV. Right: example of a third-degree polynomial fit to the values of R($\Delta\eta$) in a central bin.

RESULTS

The corrected inclusive two-particle correlation function for data and the Pythia 6 tune MC09 at 7 TeV are shown in Fig. 2. A complex structure can be observed across the full $\Delta\eta$ and $\Delta\phi$ range, the strength of which is not reproduced by the Monte Carlo.

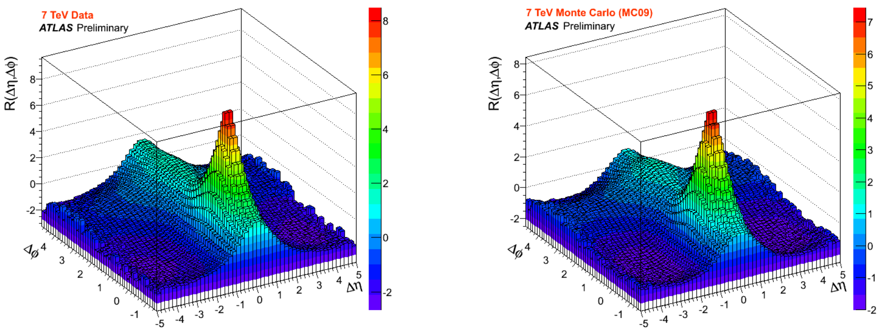

FIGURE 2. Corrected two-particle correlation distribution functions in $\Delta\eta$ and $\Delta\phi$ for 7 TeV data (left) and the MC09 tune (right).

The corrected $\Delta\eta$ correlation distributions are shown in Fig. 3, calculated by integrating $\Delta\phi$ over the limited ranges $(0 : \frac{\pi}{2})$ and $(\frac{\pi}{2} : \pi)$. The blue dots correspond to the corrected values, the blue error bars are statistical only and the green bands correspond to the total uncertainty in the bin. The data distributions are compared to different Monte Carlo tunes. By focusing on the particle pairs in the near-side $(0 : \frac{\pi}{2})$, the distributions are dominated by the peak at (0,0) so they are narrower and higher, showing a higher degree of correlations between nearby particles. Pythia 8 and Phojet have better agreement in the tails of the distribution while MC09 is closer in the peak. In the case of pairs in the away-side $(\frac{\pi}{2} : \pi)$, the distributions are flatter and wider (dominated by longer range correlations) and, with the exception of DW, the tunes seem to perform better in these distributions.

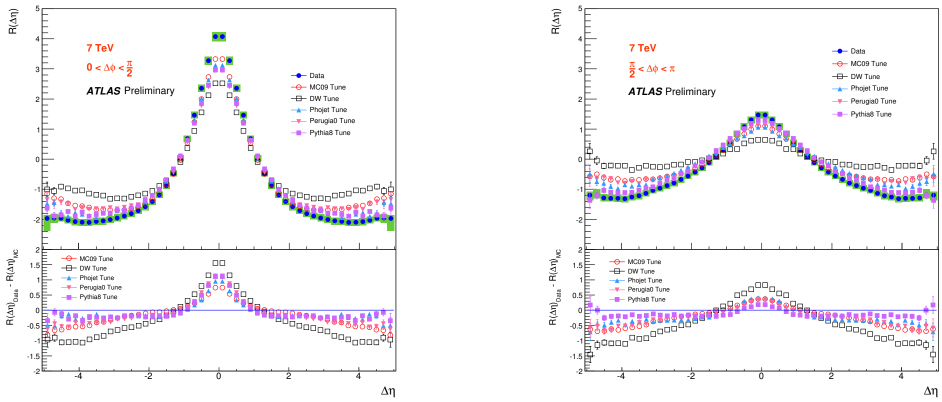

FIGURE 3. Two-particle pseudorapidity correlation distributions obtained by integrating $\Delta\phi$ from 0 to $\frac{\pi}{2}$ (left) and from $\frac{\pi}{2}$ to π (right) for 7 TeV data and the different MC tunes.

The azimuthal correlation function was studied by integrating $\Delta\eta$ over two different ranges (0:2) and (2:5). The first projection in Fig. 4 (left plot) focuses on the short-range correlations displaying an "M" shaped structure, similar to that seen in some underlying event distributions associated to back-to-back recoil phenomena. Most of the tunes agree well with data in a small region around $\Delta\phi = \pi$. The second $\Delta\phi$ projection (right plot) avoids the central peak to study the underlying structure of the long-range correlations. The absolute difference between data and the different models is flat across $\Delta\phi$. Pythia 8 is the closest and DW is the most discrepant tune with the data.

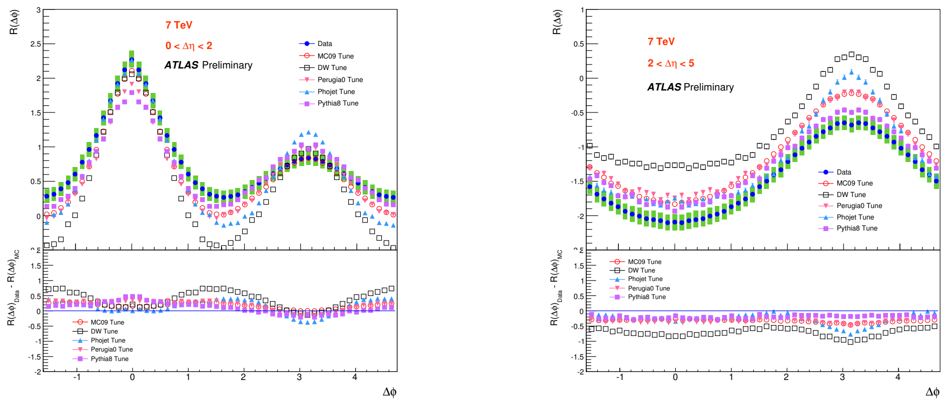

FIGURE 4. Two-particle azimuthal correlation distributions obtained by integrating $\Delta\eta$ from 0 to 2 (left) and from 2 to 5 (right) for 7 TeV data and the different MC tunes.

SUMMARY

The two-particle angular correlation function in $\Delta\eta$ and $\Delta\phi$ has been measured for p_T inclusive minimum bias events in proton-proton collisions at 7 TeV with the ATLAS Detector at the LHC. The results have been compared to Monte Carlo samples which show a similar structure but fail to reproduce the strength of the correlations seen in data.

REFERENCES

1. PHOBOS Collaboration, B. Alver et al., Phys. Rev. **C75** (2007) 054913.
2. ATLAS Collaboration, G. Aad et al., JINST **3** (2008) S08003.
3. ATLAS Collaboration, **ATLAS-CONF-2011-055** `http://cdsweb.cern.ch/record/1342570`.
4. T. Sjostrand, S. Mrenna and P. Skands, Comput. Phys. Comm. **178** (2008), `arXiv:0710.3820`.
5. R. Engel, Z. Phys. **C66** (1995) 203 - 214.
6. T. Sjostrand, S. Mrenna and P. Skands, JHEP **05** (2006) 026, `arXiv:hep-ph/0603175`.
7. M. Albrow et al., `arXiv:hep-ph/0610012`.
8. P. Skands, `arXiv:0905.3418[hep-ph]`.
9. ATLAS Collaboration, **ATL-PHYS-PUB-2010-002** `http://cdsweb.cern.ch/record/1247375`.